Available online at www.sciencedirect.com
SCIENCE DIRECT
ELSEVIER
Composites: Part B 37 (2006) 137–147
composites Part B: engineering
www.elsevier.com/locate/compositesb

Finite element continuum damage modeling of plain weave reinforced composites

E.J. Barbero[a,*], P. Lonetti[b], K.K. Sikkil[c]

[a]Mechanical and Aerospace Engineering, West Virginia University, 325 Engineering Science Building, Morgantown, WV 26505-6106, USA
[b]University of Calabria, Italy
[c]Mechanical and Aerospace Engineering, West Virginia University, Morgantown, WV 26506, USA

Received 8 January 2005; revised 19 May 2005; accepted 22 June 2005
Available online 10 August 2005

Abstract

Geometrical models needed for finite element discretization of plain-weave fabric-reinforced composites are developed from measurements taken on photomicrographs of single lamina and laminated composites. Then, a meso-level damage model is implemented into ANSYS as a user-defined material model for predicting the non-linear behavior of plain-weave reinforced laminates under tensile loading. The damage model is validated for the tensile response of T300/5208 laminate for four configurations, $[10/-10]_{2s}$, $[0/45/-45/90]_s$, $[30/-30]_{2s}$ and $[45/-45]_{2s}$. Then, the damage behavior of plain-weave fabric-reinforced laminates is analyzed using the proposed damage model in the context of the finite element method. The modes of continuum damage are identified from the analysis. Comparisons with experimental data are provided in order to support validity of the proposed models.

Keywords: A. Laminates; B. Mechanical properties; B. Microstructure; C. Damage mechanics; Finite element method

1. Introduction

Unidirectional laminated composites exhibit excellent in-plane properties, but relatively low inter-laminar properties, as they have no reinforcements in the thickness direction. This leads to relatively low damage tolerance and impact resistance. Plain weave fabrics are used as reinforcements in order to overcome these problems and to obtain balanced ply properties and improved inter-laminar properties. But these advantages are at the cost of reduced stiffness and strength in the in-plane directions. Therefore, it is important to study the mechanical behavior of such composites in order to fully realize their potential.

A fabric is a collection of fiber yarns arranged in a given pattern. Both fibers and matrix are responsible for bearing the mechanical loads while the matrix protects the fibers from environmental attacks [1]. Fabrics are classified as woven, non-woven, knitted, or braided fabrics [2]. Further, they can also be classified into 2D (two-dimensional reinforcement) and 3D fabrics (three-dimensional reinforcement). Some examples are plain weave, satin weave, weft knitted, warp knitted, and orthogonal fabrics.

The stiffness and strength depend upon the fabric architecture and material properties of fiber and matrix. The fabric architecture depends upon the undulation of the yarns, yarn crimps, density of the yarns, etc. The undulation or waviness of the yarns causes crimps (bending) in the yarns, which reduces the mechanical properties of the composite. The geometry of the woven composites is complex and the choice of possible architectures is unlimited. The present work concentrates on modeling the in-elastic behavior of the simplest of the woven fabrics—plain weave fabrics, using the finite element method and a recent damage mechanics formulation.

Plain weave fabrics are formed by interlacing (weaving) of yarns. The yarns in the longitudinal direction are known as warp yarns. The yarns in the transverse direction are known as fill yarns or weft. The interlacing causes bending in the yarns, called yarn crimp. In order to model the fabric-reinforced laminates using finite element methods, only the representative volume elements (RVE) of the respective configurations are considered. The RVE is the repeating

* Corresponding author. Fax: +1 304 293 6689.
E-mail address: ebarbero@wvu.edu (E.J. Barbero).

1359-8368/$ - see front matter
doi:10.1016/j.compositesb.2005.06.001

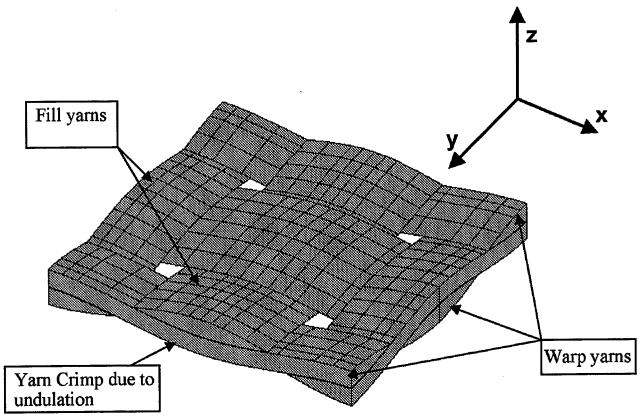

Fig. 1. Model of a single lamina without matrix.

element (unit cell) that represents the whole composite fabric structure (Fig. 1).

Although theories to model the elastic behavior of plain weave fabric composites are well understood, few theories exist to predict the non-linear behavior of such fabrics due to damage. Therefore, the objectives of this research are (a) to develop 3D finite element discretizations of plain weave laminated composites, and (b) to predict the in-elastic behavior of plain weave laminated composites under tensile loading with a damage constitutive equation programmed into a commercial program.

Numerous methods are available for modeling and analyzing plain weave fabric composites. A number of models are limited to predicting the elastic properties of the fabric reinforced composite [3–7]. The following review emphasizes models aimed at predicting strength and/or damage evolution. There are two main categories: analytical models and numerical models.

Most analytical models are based on the micromechanical study of the fabrics. Huang [8] developed a micromechanical bridging-model to predict the elastic properties and strength of woven fabric composites. The yarn cross-section is taken as elliptical and yarn undulation is described by a sinusoidal function. A discretization procedure is applied to the RVE of the fabric composite. The RVE is divided into a number of sub-elements, with no divisions in the thickness direction (Fig. 7 in [8]). Each sub-element consists of the yarn segments and the pure matrix. The yarn segments are considered as unidirectional composites in their material coordinate system. The elastic response (compliance) of the yarn segments and the matrix are assembled in order to get the effective stiffness of the sub-element using classical laminate theory (iso-strain condition). The overall elastic property of the RVE is calculated by assembling the compliance matrix of the sub-elements under iso-stress assumption. In order to calculate the strength, the fiber is assumed to be elastic until failure and the matrix is considered as elasto-plastic. The overall stress applied to the sub-element is used to obtain the global stress sustained by each yarn segment and the matrix. These stresses are then transformed to the material coordinate system for the yarn segments. Huang [8] established a relation between the stresses in the matrix and fiber in the yarn using a bridging matrix, which indicates the load share capacity of fiber with respect to matrix. Using such relation, average stresses in the fibers and matrix are calculated and compared with the individual strengths. Only the stiffness of the matrix material is non-linear as it is considered to be elasto-plastic. The tensile strength of the fabric is predicted when the average fiber stress in the yarn reaches a preset value of fiber strength.

Scida et al. [9] developed an analytical model called MESOTEX (MEchanical Simulation Of TEXtiles) based of classical lamination theory to predict the 3D elastic properties, continuum damage evolution, and strength of woven fabric composites. The properties are calculated by discretization process of the yarns and matrix in the unit cell as done by the previous investigators. The calculated stiffness is compared with experimental data and other models. Failure analysis is carried out using the Tsai-Wu criteria. The local stress in each dicretized yarn element of the unit cell is compared with the permissible values using the criteria. The Von-Mises criterion is used for predicting yield in the matrix. Once the first ply failure occurs, the ply-discount method is used to reduce the stiffness, i.e. the stiffness of the element that is subjected failure is reduced to zero. The limitation of this model is that only the in-plane stresses of the fabrics are used in the calculation of the failure in a yarn whereas inter-laminar effects are important in fabrics. Also, the ply-discount method used for stiffness reduction scheme is very approximate.

Chou et al. [10] developed 1D analytical models of the plain weave laminated composites for determining their stiffness and strength. The undulation of the fill yarn is not considered for the analysis. The undulation of the warp yarn is assumed to be sinusoidal and two types of cross-section are assumed for the fill yarns: sinusoidal and elliptical. The iso-strain condition is used for evaluating the stiffness of the plain weave laminates. In case of the strength analysis, the maximum stress criterion is used for prediction of failure strength of the laminates. The predictions correlate well with experimental results for the in-plane Young's modulus and strength values when elliptical cross-section is assumed for fill yarns.

Also, Chou et al. [11,12] developed three models to predict the damage continuum and strength of woven fabric laminates. The mosaic model [11] is used to predict the stiffness of satin weave fabric composites. The model neglects the yarn crimp and idealizes the composite as an assemblage of asymmetric cross-ply laminates. Then, iso-stress or iso-strain condition is used to predict the stiffness of the laminate depending on whether the laminates are assembled in series or parallel. Since the model neglects the yarn crimp, the prediction of stiffness is not accurate. The fiber undulation model [11] considers fiber undulation in the longitudinal direction but neglects the undulation the transverse direction. The bridging model [12], a combination of mosaic and fiber undulation model, is developed for satin weave fabrics. The model reduces to the crimp model [11] for the plain weave fabrics and hence the stiffness prediction is not accurate.

While the mathematical models described so far provide simplified stress–strain distributions, numerical models provide detailed stress–strain distributions. The geometrical description of the unit cell architecture with the yarns and matrix is the most important aspect in finite element analysis. Mathematical models have been developed to describe the geometry of a unit cell.

Blackletter et al. [13] developed a 3D finite element model of a plain weave fabric and studied the damage continuum propagation in the fabric under tensile and shear loading. The yarns and matrix are modeled using PATRAN. Hexahedral elements are used for generating the mesh. The yarns are modeled as unidirectional composite materials. The yarn properties are calculated using two-dimensional generalized plane strain micromechanics analysis. The properties of individual fibers and matrix are used for predicting the damage behavior of the yarns used in the failure analysis. In the in-elastic analysis, the damage is tracked at each Gaussian integration point. The maximum normal stress criterion is used for the matrix elements, i.e. when the principal stresses exceed the strength values; the tensile modulus and shear modulus are degraded by a fudge factor in the range 0.01–0.1. Maximum stress criterion is used for the yarn elements, i.e. when the stress in the material coordinate exceeds the ultimate strengths; the stiffness is reduced in the appropriate direction at each integration point. The damage model is then used in finite element analysis to predict the in-elastic behavior of plain weave fabrics. Transverse failure is observed prior to catastrophic failure of the fabric in the tensile test. The model over-predicts the failure strength of the fabric. In the case of the shear test, transverse tensile failure of the yarns is observed which, according to the model, results in reduction of transverse tensile modulus and in-plane shear modulus to essentially zero. But, the analysis greatly under predicts the failure strength. Therefore, the degradation factor of in-plane shear modulus is assumed as 0.2 instead of 0.01 so as to match the experimental shear response. Therefore, the damage model employed is similar to the degradation factor method [1] and it is therefore approximate and dependent on the laminate stacking sequence (LSS) and other factors [14].

Sridharan et al. [15,16] developed two types of finite element model for plain weave fabrics. The first type is similar to the previous finite element models where the quarter model of the RVE, containing the yarns and matrix, is meshed using 3D solid elements. The second type is different from the usual models. Here, the model consists of plate elements representing the yarns and 3D solid elements representing the matrix sandwiched between the yarns. Thus, the unit cell consists of four plate elements representing fill and warp yarns. The thickness variations in the yarns are incorporated in the plate elements. Continuum damage responses of the two models match well with the experimental data. The continuum damage analysis of the models is carried out by assuming material non-linearity in the yarns and matrix. A micromechanical model is used in order to describe the stress state of fiber and matrix within the yarns. The fibers are assumed to be elastic until failure. The micromechanical model is re-calculated at each integration point for all iterations and thus it is computationally expensive. The non-linearity of the matrix is modeled using Ramberg–Osgood relations. Also, non-linear geometry is considered for the analysis. The inelastic behavior of plain weave fabrics is analyzed when subjected to in-plane tensile, compressive, and shear loads applied in the fill direction. The model identifies the failure modes for each loading. The model gives a good strength prediction for plain weave laminates subjected to tension and shear.

Although a number of plain weave fabric models are available for predicting stiffness and strength, each model has their limitations. Therefore, the aim of this work is to develop a novel finite element representation of plain weave fabrics based on geometrical measurements from photomicrographs and to determine the damage evolution using a meso-mechanical continuum damage formulation.

2. 2D geometrical models

The geometrical model for the representative volume element (RVE) and the yarns for plain weave fabrics were developed using the geometrical parameters measured by Ito and Chou [10]. The RVE consists of four intertwined yarns surrounded by the isotropic matrix. There are two warp yarns in the longitudinal direction and two fill yarns in the transverse direction. Each yarn is a unidirectional composite in the material coordinate system with orthotropic properties. 2D and 3D views of the fabric are shown in Figs. 2 and 3.

The 2D geometrical model describing the internal geometry of the RVE of a single lamina is developed from the values measured on the photomicrographs of the faces of the RVE, one of which is shown in Fig. 2 [17,18]. The parameters describing the geometry are shown in Fig. 4.

The equations proposed by Ito and Chou [10] for the yarn geometry on the faces of the RVE are used as a starting point for developing the geometrical model for each kind of laminate. The warp yarn path curve on the fill face of the RVE is described by

$$y = \frac{b}{2}\sin\left(\frac{2\pi x}{a}\right), \quad \text{where} \quad -\frac{a}{4}<x<\frac{a}{4} \tag{1}$$

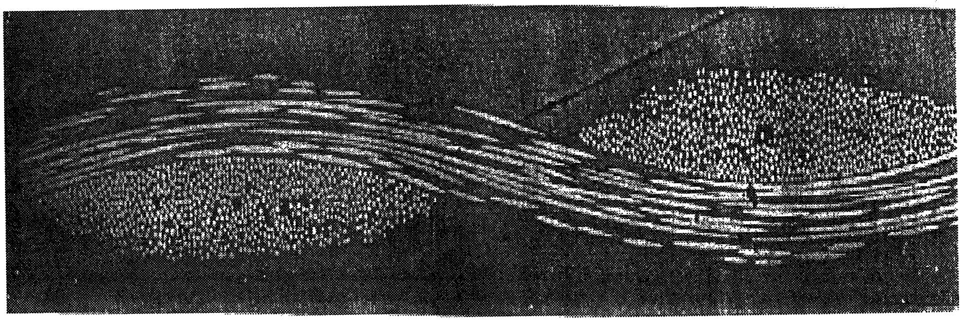

Fig. 2. 2D photomicrograph of the plain weave fabric.

and the fill yarn cross-section curve on the same face by

$$y = \left(\frac{2hc}{a-2ag}\right) \times \sqrt{(2x-ag)(a-ag-2x)} + b - hc, \quad (2)$$

where $\frac{ag}{2} < x < \frac{a}{4}$

where $hc = b/2(\sin(\pi a_g/a) + 1)$, b is the yarn thickness, a is the dimension of the RVE in either the fill or warp directions (warp or fill faces, respectively), and a_g is the gap between two adjacent yarns. The values of the parameters are shown in Table 1.

3. 3D geometric modeling

The 3D geometric models are created using I-DEAS, Version.8, which is chosen because it is simple, has interactive GUI menus that are easy to work with, and offers features like creating volumes from set of curves, partitioning of solids, material orientation features, etc.

The procedure for developing 3D geometric models of a single lamina based on the 2D geometrical model is the following. First, the yarn path curves and the yarn cross-section curves in the warp and fill directions are drafted from the measured parameters (Table 1), and equations (Eqs. (1)–(2)) using the function spline option in I-DEAS. Sweeping operation could not be performed with the curves because the warp (and fill) yarn cross-section curves do not necessarily match the fill (and warp) yarn path curves in the faces of the RVE. This is due to the fact that the fill and warp cross-section and path curves may have different shape (e.g. $a^{w} \neq a^{f}$; $a_g^{w} \neq a_g^{f}$ in Table 1). Therefore, a separate description for the warp and fill geometry is necessary [18]. So, the cross-section curves need to be blended with the path curve. For this purpose, the cross-section curves are flipped (rotated by 180°) in the faces of the RVE where the cross-section curves do not match the path curves. Then, the surfaces are formed from the cross-section and path curves that define the yarn surfaces in the warp and fill directions. In order to define the surfaces of warp or fill yarns, three path curves and four cross-section curves are required. Surfaces related to the warp (and fill) are stitched together to get a solid model of the yarns. In total, the four intertwined yarns are formed with two of them in the warp direction and two in the fill direction. But there is a problem of yarns intersection when the surfaces are stitched together. This is due to interpolation of I-DEAS software when the surfaces are formed from the (analytical) spline curves. So, the fill yarns are slightly rotated about the warp axis to make the four yarns non-intersecting, which resulted in a small gap between them. This small gap is modeled as matrix. The yarns are then partitioned from a rectangular prism having the dimensions the RVE, which indicates to

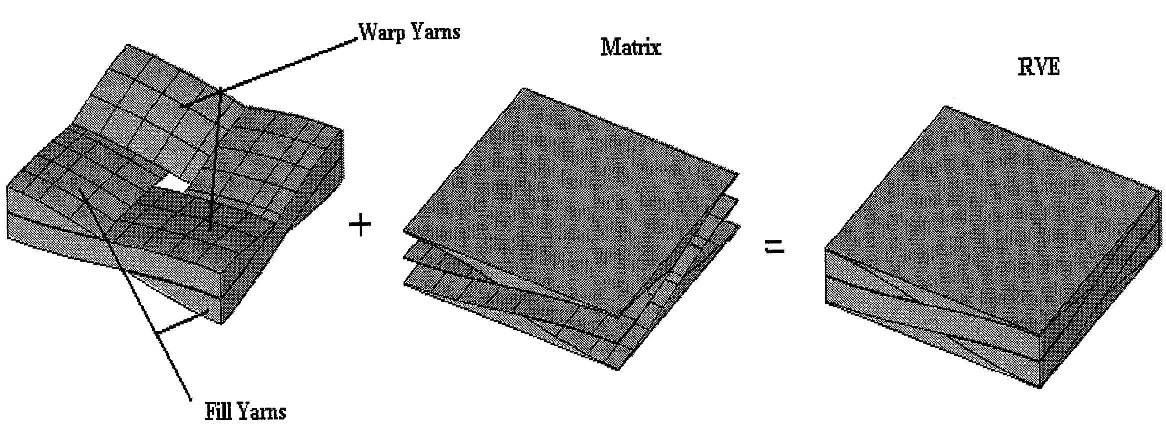

Fig. 3. 3D views of a plain weave fabric.

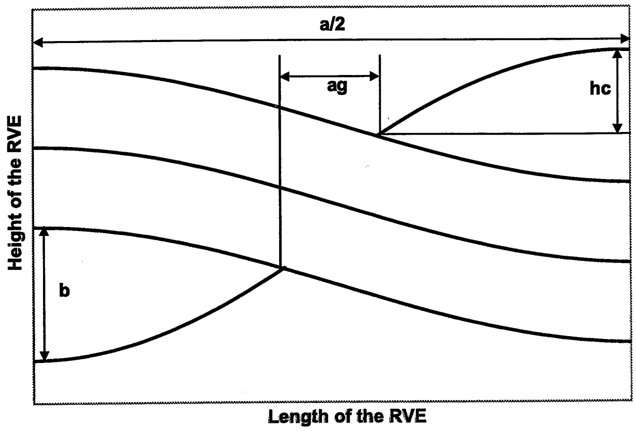

Fig. 4. Yarn parameters measured by Ito and Chou [10].

the software that there are four yarns inside the prism. This is visualized as four yarns surrounded by matrix as shown in Fig. 3.

In addition to measuring the yarn parameters of a single lamina, Ito and Chou also measured the parameters for fabric-reinforced laminates [10]. In this work, the number of plies modeled is eight, the same used in the experiment [10]. So, copies of the single lamina are made and moved by an amount equal to the thickness of the lamina (Table 1). Then, the join operation is used to join the eight laminates. The finite element discretizations are developed from the geometric models by automatic free meshing as explained in Section 4.

4. Finite element discretization

The 3D geometric models are meshed using 10 node solid parabolic tetrahedral elements under the free mesh option in I-DEAS. Each node has three degrees of freedom, u_x, u_y and u_z. The elements exhibit a quadratic displacement behavior, which is well suited for modeling the complex and irregular structure of the plain weave fabric. The mesh is checked for distortion.

A mesh sensitivity analysis is performed in order to get accurate results. The material property of the yarns varies along the orientation of the yarn curve. Therefore, the material orientations of yarn elements are made to follow the yarn curve using the material orientation option. The local X-direction of the coordinate system for each element follows the path curves of the warp or fill yarns (depending on the yarns for which material orientation is being defined). The X-direction of the yarn elements indicates the fiber direction, the Y-direction indicates the transverse direction of the RVE and the Z-direction indicates the thickness direction (Fig. 5).

Table 1
Geometrical parameters measured by Ito and Chou [10]

Geometrical Parameters	Single lamina and laminate
Weave length in warp direction, a^{w} (mm)	6.432
Gap width in warp direction, $a_{\mathrm{g}}^{\mathrm{w}}$ (mm)	0.392
Weave length in fill direction, a^{f} (mm)	6.11
Gap width in fill direction, $a_{\mathrm{g}}^{\mathrm{f}}$ (mm)	0.275
Yarn thickness, b (mm)	0.318

Transversely isotropic material properties are assigned to the yarn elements and isotropic properties are assigned to the matrix elements. The material properties of the yarns are calculated using micromechanics [19,20] depending on whether the fibers are isotropic or transversely isotropic.

The overall volume fraction (V_{o}) is obtained from experimental data [10] for the three laminate configurations and it is reported in Table 2. Experimental values of V_{o} can be obtained from ignition loss method (ASTM D2854), acid digestion (ASTM D3171) or solvent extraction (ASTM C613). V_{o} is the product of the meso-scale volume fraction V_{meso} and yarn volume fraction V_{f}. The meso-scale volume fraction can be obtained from the solid model as the ratio of yarn volume to RVE volume

$$V_{\mathrm{meso}}=\frac{\Delta_{\mathrm{yarn}}}{\Delta_{\mathrm{rve}}} \tag{3}$$

Therefore, the microscale (yarn) volume fraction can be obtained as

$$V_{\mathrm{f}}=\frac{V_{\mathrm{o}}}{V_{\mathrm{meso}}} \tag{4}$$

where V_{meso} is the meso-scale volume fraction obtained from the geometric model, V_{f} is the microscale fiber volume fraction used for calculating the material properties of the composite yarns, Δ_{yarn} is the total volume of the yarns calculated from the geometric model, and Δ_{rve} is the volume of the RVE obtained from the geometric model. The yarn fiber volume fraction V_{f} calculated from Eq. (4) did not match the V_{f} reported in [10] because V_{meso} from our model is too high due to the rotation of the yarns that results in a slight artificial increase in thickness of the RVE. This is accounted for by calculating the correct meso-scale volume fraction V'_{meso} using the original dimensions of RVE, as follows

$$V'_{\mathrm{meso}}=\frac{\Delta_{\mathrm{yarn}}}{\Delta'_{\mathrm{rve}}} \tag{5}$$

and recalculating the yarn fiber volume fraction

$$V'_{\mathrm{f}}=\frac{V_{\mathrm{o}}}{V'_{\mathrm{meso}}} \tag{6}$$

where V'_{meso} is the corrected meso-scale volume fraction from measured data [10], Δ'_{rve} is the corrected volume of RVE from measured data [10], and V_{f}' is the corrected fiber volume fraction of fiber. Using V_{f}', the material properties of the yarns are calculated using micromechanics. Since AS4 carbon fiber is transversely isotropic, the elastic properties are calculated using periodic microstructure micromechanics for transversely isotropic fibers (PMM) [20].

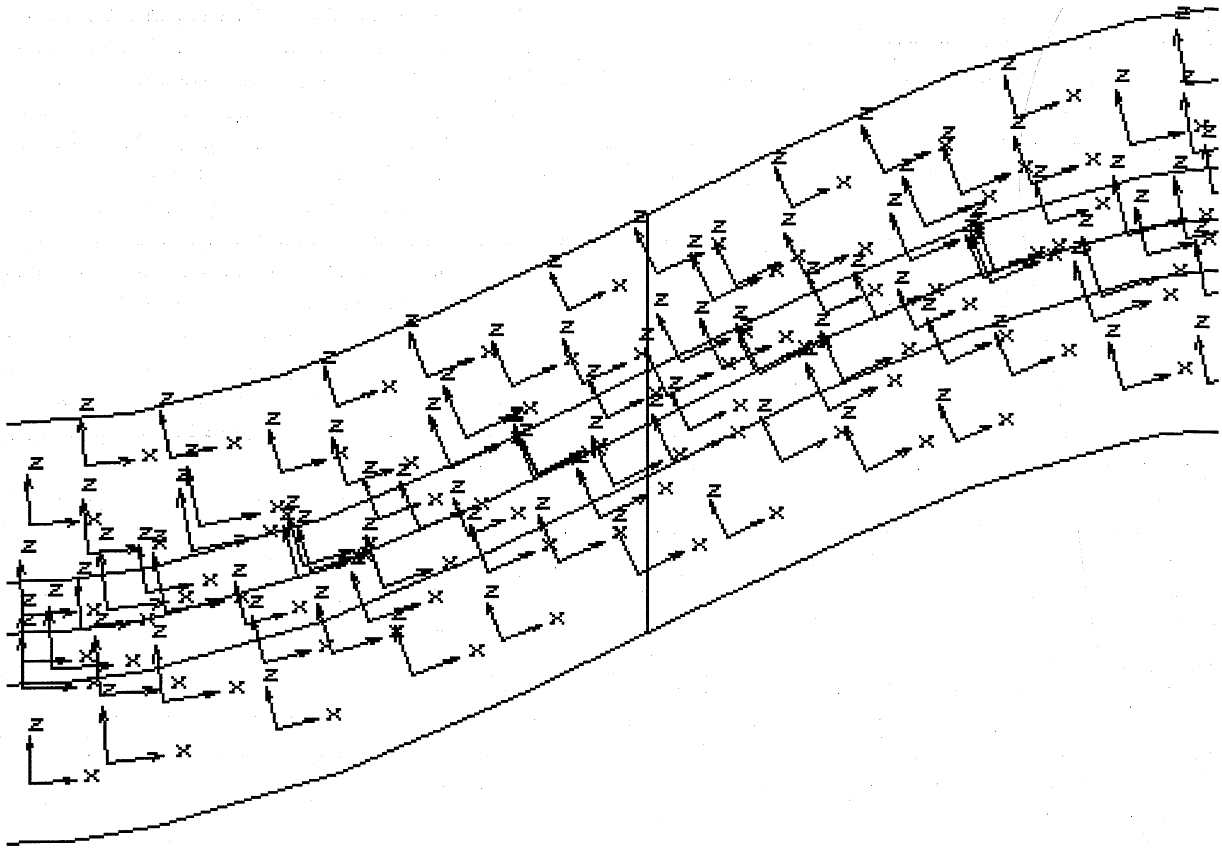

Fig. 5. Material orientation inside the yarns.

The elastic properties of constituent materials are obtained from [10]. The yarns are transversely isotropic and thus require only five properties (E_1, E_2, G_{12}, ν_{12}, ν_{23}). Then, the properties are assigned to the yarn and matrix elements in I-DEAS. The next step is to apply the boundary conditions and analyze the results.

5. Boundary, periodicity, and compatibility conditions

Only one-quarter of the RVE is modeled because the laminated plain weave fabrics are symmetric and periodic in all three directions. So, symmetric boundary conditions are assigned to the nodes at the back surfaces in the warp direction (*YZ* plane) and to the nodes at the left surfaces in the fill direction of the RVE (*XZ* plane, Fig. 1). Compatibility of displacements at the other two faces of the RVE (*YZ* and *XZ*) with the adjacent (not modeled) cells are enforced by constraint equations resulting in a plane remaining plane and having a uniform displacement on those faces [21]. Then, a uniform displacement is assigned to the nodes in the *X*-direction at the front surfaces in the warp direction to simulate a uniform strain.

Table 2
Overall, meso-scale, microscale fiber volume fraction

Volume fraction type	Volume fraction value
Overall	0.44
Meso-scale	0.65
Microscale	0.68

A linear static analysis is performed on the FE models with the necessary boundary conditions in I-DEAS. The following procedure is used for calculating the stiffness of both the single-lamina and laminated composites. During the post processing stage, the results of the reaction forces in the *X*-direction are obtained. For calculating the value of stiffness (E_x), the sum of the reaction forces (F_x) in the *X*-direction, in the loading surface of the RVE is obtained. Taking F_x and dividing it by the cross-section area of the RVE, the average stress acting on the surface is calculated (σ_x). Finally, E_x was obtained by dividing σ_x with the strain (ε). But the value has to be adjusted due to the volume fraction correction described in Eqs. (5)–(6). The actual stiffness is calculated as follows

$$E'_x = E_x\left(\frac{V'_{\text{meso}}}{V_{\text{meso}}}\right) \tag{7}$$

The predications are compared with the experimental stiffness [10] in Table 3.

Since the damage constitutive equation can be programmed as a user material subroutine in ANSYS but not in I-DEAS, the FE models of the plain weave fabric are

Table 3
Comparison of predicted and experimental stiffness E_x

Model type	Type of laminate	Ito and Chou (Experimental)	FE results
Ito and Chou [10]	Single lamina	N/A	32.8 GPa
	Laminate	42.8 GPa	41.5 GPa

exported to ANSYS, Version 6.1 as a data file. While exporting, the element type is changed to Solid 92, which is an equivalent for parabolic element in ANSYS. There were several errors encountered while opening the file in ANSYS. The ANSYS software supports two types of Poisson's ratio, major Poisson's ratio and minor Poisson's ratio, for orthotropic material model. The major Poisson's ratio (PRXY, PRYZ, PRXZ) corresponds to ν_{xy}, ν_{yz}, ν_{xz} as input. The minor Poisson's ratio (NUXY, NUYZ, NUXZ) corresponds to ν_{yx}, ν_{zy}, ν_{zx} as input. When the file is exported from I-DEAS, ANSYS interpreted ν_{xy}, ν_{yz}, ν_{xz} as minor Poisson's ratio instead of major Poisson's ratio. This resulted in error when the software verified for the restrictions on elastic constants. This is corrected by substituting PR for NU in ANSYS command lines. Once the errors are corrected, the model is solved using linear elastic behavior and the predicted laminate stiffness, E_x, is in good agreement to that using I-DEAS.

6. Damage model

Several models are available for predicting the damage behavior of composites prior to failure. Ply discount methods are very approximate methods and the predicted damage behavior is not accurate [14]. Micromechanical models are used to predict the damage behavior of a single ply by assembling the damage response of the constituent materials [22]. They are computationally intensive and require large number of material parameters. Continuous damage mechanics (CDM) models require only a few parameters to describe the damage behavior of a composite material. In most of the CDM models available in the literature, the parameters have to be obtained from non-standard and special tests, which make them expensive [23]. In this work we use a model based on available data (stiffness and strength values) using the concept of continuous damage mechanics coupled with thermodynamics [24–27]. The damage model accounts for damage initiation, evolution, and failure at critical values of damage in a composite material. The model uses a set of internal variables to describe the damage behavior. The simplicity of the model lies in the fact that only a few parameters are required for describing the non-linear behavior and they can be obtained from standard tests of a unidirectional ply.

The damage domain lies between the virgin undamaged states of the material and the macroscopic crack initiation [28]. Beyond this lies the domain of fracture mechanics. Damage in composite materials are in the form of matrix cracks, voids, fiber–matrix debond, fiber breakages, and transverse cracks, which takes place either in parallel or normal to fiber direction. In CDM, all these modes of failure are represented by a smaller, equivalent set of (continuum) damage modes. In this work, the continuum damage modes are the equivalent density of microcracks (d_1,d_2,d_3) in three orthogonal planes. Therefore, a second-order symmetric damage tensor D is used to describe the anisotropic evolution of damage along matrix and fiber directions. Since the damage principal directions are assumed to be coincident with the material directions [27], a diagonal, second-order damage tensor D is used, with diagonal terms d_1, d_2, d_3 representing the net area reduction along the three material directions.

Since the damage model is set in the thermodynamic framework, the second-order symmetric tensor **Y**, dual to the damage tensor D is given by

$$Y = -\frac{\partial \Phi}{\partial D} = -\frac{1}{2}\sigma\frac{\partial}{\partial D}(M^{-1}(\bar{E})^{-1}M^{-1})\sigma \tag{8}$$

where Φ is the strain energy potential, $\bar{E}$ is the undamaged stiffness tensor, and **M** is the fourth-order damage effect tensor [27]. The damage surface, which is analogous to the yield surface in plasticity theory, is given by

$$g^d = (Y : J : Y)^{1/2} + (|H : Y|)^{1/2} - \gamma(\delta) - \gamma_0 \tag{9}$$

where **Y** is the thermodynamic force tensor, **J** and **H** are the tensors of the internal material constants, $\gamma(\delta)$ is the damage evolution variable, and γ_0 is the damage threshold representing the initial size of the damage surface.

No damage occurs until the thermodynamic forces **Y** reach the damage surface. For undamaged material, $\gamma = 0$, and g^d has the shape of the Tsai-Wu surface. At failure, $\gamma^* + \gamma_0 = 1$ and the shape and size of g^d matches the Tsai-Wu surface where γ^* represents the value of γ at failure. Comparing the two surfaces, we arrive at a set of a linear system of equations that allow us to determine the internal material constants univocally in terms of known material properties [24–27]. Hardening of the damage surface takes place according to [24]

$$\gamma(\delta) = c_1[\exp(\delta/c_2) - 1] \tag{10}$$

The damage evolution parameters (c_1, c_2) and the damage threshold (γ_0) are calculated by adjusting the shear stress–strain obtained from finite element analysis of a unidirectional ply subjected to pure shear conditions to match the experimental shear response.

The internal material constants are related to the experimental properties. They are calculated based on the set of equations as discussed below, using a program written in MAPLE, Version 5 [18].

The input variables required for calculating the material constants are the following. The stiffness values (E_1, $E_2 = E_3$, $G_{12} = G_{13}$, G_{23}, ν_{12}) of the composite material, the strength values of the composite in tension (F_{1t}, F_{2t}), compression (F_{1c}) and shear (F_4, F_5, F_6), the critical damage values in tension (D_{1t}), compression (D_{1c}), transverse tension (D_{2t}), and the damaged shear modulus at failure (G_{12}^*, G_{13}^*, G_{23}^*).

The input variables are calculated as follows. For transversely isotropic materials, only five properties are required (E_1, E_2, G_{12}, ν_{12}, ν_{23}). The properties are computed using periodic microstructure model (PMM [20]). The strength values are obtained from uniaxial experimental tests of unidirectional composites. If the strength data is not available, empirical relations are used for calculating the strength values [1]. The critical damage values are obtained for a unidirectional laminate. D_{1t} is critical damage value for longitudinal tensile loading and it indicates the area fraction of broken fibers at the onset of longitudinal tensile failure. D_{1c} is the critical damage value for longitudinal compressive loading and it indicates the area fraction of fibers buckled at the onset of longitudinal compressive failure. D_{2t} is the critical damage value for transverse tensile loading and it indicates the area fraction of broken matrix links at the onset of transverse tensile failure. The critical damage values for D_{1t}, D_{1c}, DD_{2t} are obtained from [25]. The damaged shear modulus can be approximated as the ratio of shear strength to the ultimate strain at failure assuming elastic unloading to the origin. If unrecoverable (plastic) strains occur, damaged moduli must be obtained from the unloading portion of the stress–strain plot.

The internal constants are defined by fourth and second order tensors **J** and **H**, respectively. They appear in the formulation of the damage surface g^d (Eq. (9)) in thermodynamic force space, which represents the Tsai-Wu surface in stress space at failure. Since the principal directions of the damage tensor coincides with the material directions, the **J** and **H** tensors are diagonal. The six coefficients in the **J** and **H** tensors are calculated from experimentally known properties as described in [18,25].

The hardening parameters c_1, c_2, control the damage evolution. The damage threshold γ_0 represents the initial size of the damage surface. Since the material behavior is highly non-linear for a composite lamina for in-plane shear mode, as indicated from experimental observations, the damage is assumed to be notable in this case [25]. Therefore, c_1, c_2 and γ_0 are adjusted to predict the experimental shear response of the lamina subjected to pure shear conditions using Finite Element Analysis. In case the experimental shear plot is not available for a material, but only G_{12} and F_6 are known, the curve can be determined using the empirical relation [1]

$$\sigma_6 = F_6 \tanh\left(\frac{G_{12}}{F_6} 2\varepsilon_6\right) \tag{11}$$

The finite element model is then subjected to pure shear condition [18]. During the post-processing stage, the sum of the reaction forces (F_{xy}) in the in-plane shear direction and the deformation in the front faces of the lamina are recorded for each substep. The average shear stress is calculated by dividing F_{xy} by the shear area and the shear strain is calculated from the deformation of nodes in the front face of the RVE. The shear stress–strain from the analysis is plotted and compared to the experimental shear response. If the curves do not match, then the values of c_1, c_2 and γ_0 are adjusted and the procedure is repeated until the shear stress–strain plot matches the experimental shear response.

In order to include material non-linearity, a user subroutine is written in FORTRAN and linked with ANSYS [29]. The procedure is explained in [18]. A customized ANSYS executable is obtained from this procedure. A single lamina is modeled in I-DEAS and meshed using 20-noded solid brick elements. The finite element model is then exported to the user defined ANSYS. The equivalent element in ANSYS is Solid186, which allows user material properties to be defined. The material properties and parameters are input in the ANSYS user-material model definition. A mesh sensitivity analysis is performed in order to get accurate results. The non-linear analysis is run with optimum number of substeps.

7. Damage analysis of plain weave fabrics

The FE models of fabric-reinforced laminates developed in IDEAS™ are exported to user-defined ANSYS™ as input files. The equivalent element in ANSYS is Solid187 that is used to incorporate the user material model into the analysis. In order to perform the tensile test, symmetric and compatibility conditions are applied to the sides surface of the RVE and uniform strain is applied to the front side of the RVE as explained before. The damage model is applied only to the yarns and the matrix is assumed to be elastic. Here, both in-plane and inter-laminar stresses are taken into consideration. The parameters of the damage model for AS4/vinyl ester yarns are obtained as follows:

The elastic properties of AS4/vinyl ester computed using periodic micro mechanics model (PMM) [20] are obtained from Table 4. The transverse tensile strength F_{2t} and inter-laminar strength F_5 are available from [10]. The longitudinal tensile strength F_{1t} is calculated using the strength of the AS4 fiber (3930 MPa) available in [10] and Eq. 4.59 from [1]. F_5 is assumed to be same as F_6. F_4 is assumed to be 50 MPa. F_{1c} is obtained using the empirical relation (Eq. 4.75 in [1])

$$F_{1c} = \left(\frac{\chi}{a} + 1\right)^b G_{12}; \qquad \chi = \frac{G_{12}\Omega}{F_6} \tag{12}$$

where Ω is the standard deviation of the Gaussian distribution of fiber misalignment, a, b are constants [1], G_{12} is the in-plane shear modulus, and F_6 is the in-plane shear strength. In case of the fabrics, the fiber misalignment is more than that of a unidirectional fiber tow because

Table 4
Elastic properties of the fiber, yarn and matrix

Fiber (Carbon: AS4)	$E_{f1}=221$ GPa, $E_{f2}=16.6$ GPa, $\nu_{12f}=0.26$, $G_{12f}=8.27$ GPa, $G_{23f}=5.89$ GPa
Matrix (vinyl ester)	$E_m=3.4$ GPa, $\nu_m=0.3$
Yarn (carbon/vinyl ester), $V_f=0.69$	$E_1=151.36$ GPa, $E_2=9.04$ GPa, $\nu_{12}=0.27$, $G_{12}=3.89$ GPa, $G_{23}=3.36$ GPa

the yarns are twisted. Therefore, a high value of standard deviation $\Omega=2.8°$ is assumed [30]. The critical damage values D_{1t}, and D_{2t} are obtained from [24]. The longitudinal compressive critical damage D_{1c} for a plain weave is higher than that for a unidirectional laminate because of the fiber misalignment, and it is calculated as follows

$$D_{1c} = 1 - \mathrm{erf}\left(\frac{\alpha_{cr}}{\Lambda\sqrt{2}}\right) \tag{13}$$

where erf is the error function, α_{cr} is the critical misalignment angle at failure (Eq. (23) in [30]) and Λ is the standard deviation of the Gaussian distribution of fiber misalignment. The unloading damaged shear moduli (G^*_{12}, G^*_{13}, G^*_{23}) are calculated assuming the ultimate shear strain to be 3%. The internal constants J_{11}, J_{22}, J_{33}, H_1, H_2, H_3 are calculated from [24]. The hardening parameters (c_1, c_2) and damage threshold (γ_0) are adjusted by matching the in-plane shear response of AS4/vinyl ester composite obtained using the damage model vs. the experimental shear plot.

The material properties and the damage parameters of AS4/vinyl ester are reported in Tables 5 and 6. The non-linear analysis is performed with optimum number of substeps. The damage growth is tracked at each integration point. As the damage in the elements increase, the stiffness of the element decreases in accord to the respective continuum damage mode.

The results obtained for the damage analysis of the laminate are shown in Fig. 6. The linear curve indicates the case for which there is no damage considered for the analysis. This condition is achieved by specifying a large value for the damage threshold ($\gamma_0=1E20$), which means that the initial damage surface is very large and hence no damage occurs.

Table 5
Elastic properties of AS4/vinyl ester material

Property	AS4/vinyl ester
E_1 (MPa)	1.51×10^5
E_2 (MPa)	9040
G_{12} (MPa)	3900
G_{23} (MPa)	3360
ν_{12}	0.272
F_{1t} (MPa)	2690
F_{1c} (MPa)	630
F_{2t} (MPa)	60
F_4 (MPa)	50
F_5 (MPa)	80
F_6 (MPa)	80
G_{12} damaged (MPa)	2857
G_{13} damaged (MPa)	2652
G_{23} damaged (MPa)	1310

The damage model predicts the in-elastic experimental curve until 8400 microstrains. The model predicts that the transverse damage d_2 reaches its critical value d_2=D2cr at 7480 microstrains, which corresponds to a stress level of 275 MPa. This event is close to the initiation of macrocracks, observed experimentally to take place at 281 MPa [10].

The sequence of failures in the laminate for the loading in longitudinal direction (Figs. 6 and 7) is as follows. First, transverse tensile failure in the fill yarns occurs. Then, inter-laminar failures between the fill and warp yarns occurs. Finally, fiber damage in the warp yarns occurs.

Table 6
Damage parameters of AS4/vinyl-ester material

Property	AS4/vinyl esther
J_{11}	0.0028070
J_{22}	0.0454383
J_{33}	0.05646
H_1	0.103237
H_2	−0.0323228
H_3	0.05052
k_{s12}	0.732
k_{s13}	0.65
k_{s23}	0.31
r_{s12}	0.31309
r_{s13}	0.44575
r_{s23}	1.4237
D_{1t}	0.1161
D_{1c}	0.207
D_{2t}	0.5
D_3^{cr}	0.5
c_1	0.2
c_2	−0.65
γ_0	0.1

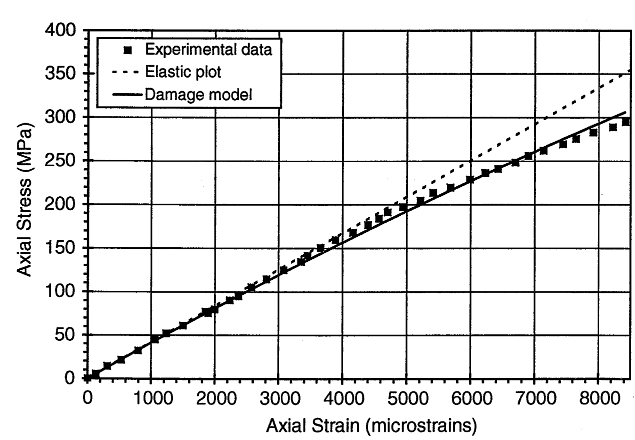

Fig. 6. Stress–strain plot for the fabric-reinforced laminate.

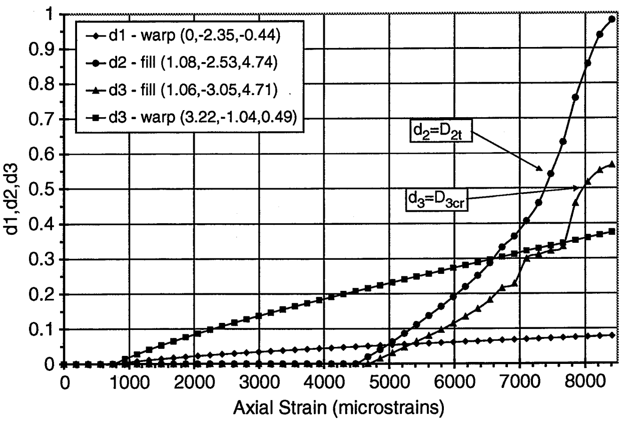

Fig. 7. Damage evolution in the model at location indicated in the parenthesis.

In order to illustrate the evolution of damage, the damage state variables (d_1,d_2,d_3) that represent the continuum damage modes are plotted against the axial strain for each sub-step of the analysis as shown in Fig. 7. The plot is indicative of the damage evolution and growth in the model. The damage variables are chosen at integration points where they are maxima. The numbers in the parenthesis indicate the location of the point in the RVE where the damage value is maximum. The coordinates of the location are with respect to the origin of the RVE. In Fig. 7, the plot for d_1 shows that the maximum value of damage is $d_1=0.078$ at a gauss point in the warp yarn (see Fig. 1 where 'warp' and 'fill' yarn are labeled). Since the warp yarn takes up most of the applied load, which is applied in the warp direction, the fibers undergo significant damage, but the damage value is less than the critical value in the longitudinal direction ($D_{1cr}=0.116$). The plot for d_2 shows that the maximum value of damage reaches the critical value $D_{2cr}=0.5$ at gauss point in the fill (transverse) yarn at 7480 microstrains. The reason it occurs in the fill yarns is because the load is applied transversely to the fill yarn (along the warp direction). Therefore, the transverse tensile stress in the fill yarn exceeds the transverse tensile strength in the local coordinate system. The stress is redistributed once the stiffness is reduced.

The inter-laminar damage variable d_3 is plotted for both fill and warp yarns. When the laminate is subjected to a uniform tensile strain along the warp direction, the sinusoidal warp yarns try to become straight. During the process of straightening, the yarns tend to twist, as they are not free to just straighten due to the interference of the fill yarns. Also, the fill yarns are twisted to some extent when warp yarns straighten. Because of twisting, the inter-laminar effect becomes important. In case of an integration point in the fill yarn element right next to the fill/warp interface, the interlaminar damage d_3 reaches its critical value $D_{3cr}=0.5$ at a stress level of 294 MPa. When the critical damage value is reached in inter-laminar direction, the model predicts the appearance of a macrocrack at a stress level of 294 MPa, while Ito and Chou [10] observed initiation of interfacial debonding between the yarns at a stress level of 281 MPa. It can be seen that inter-laminar damage has a significant effect on the strength of the laminate and the model predicts the appearance of a macrocrack at the same location and similar load as observed experimentally [10]. The maximum value of d_3 for an integration point in the warp yarn is only $d_3=0.374$, so no macrocrack appears in the warp yarns, which also agrees with experimental observations in [10].

8. Conclusions

A novel procedure is developed for finite level discretization of the yarn and matrix geometry in single-lamina and laminated fabric reinforced composites. The elastic modulus (E_x) of the plain weave laminate under tension is obtained using finite element analysis. The values predicted by the FE model compare very well with the experimental values [10]. A meso-scale damage model for predicting the in-elastic behavior of composite laminates is implemented in ANSYS. The damage model is validated for T300/5208 composite with different material orientations. The model accurately predicts the shear response of T300/5208 for $[10/-10]_{2s}$, $[0/45/-45/90]_s$, $[30/-30]_{2s}$ and $[45/-45]_{2s}$ lay-ups. The damage model predicts correctly the in-elastic curve for each lay-up due to damage. The damage of fabric-reinforced laminate is also accurately predicted. At a stress level of 294 MPa, the proposed model predicts the appearance of a macrocrack, in good agreement with experimental observations. The proposed methodology relies on identifying the damage parameters at the lamina level. This is a limitation in that any change in the fiber volume fraction of the material needs a new set of tests to be performed in order to identify the new values for the damage parameters.

Acknowledgements

Thanks to Dr Joan Andreu Mayugo of University of Girona, Spain, for his collaboration in setting up the periodicity conditions on the models.

References

[1] Barbero EJ. Introduction to composite materials design. Philadelphia, PA: Taylor and Francis; 1999.

[2] Pandey R. Micromechanics based computer-aided design and analysis of two-dimensional and three-dimensional fabric composites Dissertation. PA: Pennsylvania State University; 1995.

[3] Naik NK, Ganesh VK. Prediction of on-axes elastic properties of plain weave fabric composites. Compos Sci Technol 1992;45:135–52.

[4] Vandeurzen Ph, Ivens J, Verpoest I. A three-dimensional micro-mechanical analysis of woven-fabric composites. I. Geometric analysis. Compos Sci Technol 1996;56:1303–15.

[5] Vandeurzen Ph, Ivens J, Verpoest I. A three-dimensional micromechanical analysis of Woven-Fabric composites: II. elastic analysis. Compos Sci Technol 1996;56:1317–27.
[6] Hahn HT, Pandey R. A micromechanics model for thermo-elastic properties of plain weave fabric composites. J Eng Mater Technol 1994;116:517–23.
[7] Aitharaju VR, Averill RC. Three-dimensional properties of Woven-Fabric composites. Compos Sci Technol 1999;59:1901–11.
[8] Huang ZM. The mechanical properties of composites reinforced with Woven and Braided fabrics. Compos Sci Technol 1999;60:479–98.
[9] Scida D, Aboura Z, Benzeggagh ML, Bocherens E. A micromechanics model for 3D elasticity and failure of Woven-Fiber composite materials. Compos Sci Technol 1999;59:505–17.
[10] Chou TW, Ito M. An analytical and experimental study of strength and failure behavior of plain weave composites. J Compos Mater 1998;32:2–30.
[11] Ishikawa T, Chou TW. One-dimensional micromechanical analysis of Woven fabric composites. J Am Inst Aeronaut Astronaut 1983;21:1714–21.
[12] Ishikawa T, Chou TW. Stiffness and strength behavior of Woven fabric composites. J Mater Sci 1982;17:3211–20.
[13] Blackletter DM, Walrath DE, Hansen AC. Modeling damage in a plain weave fabric-reinforced composite material. J Compos Technol Res 1993;15:136–42.
[14] Kim Y, Davalos JF, Barbero EJ. Delamination buckling of FRP layer in laminated wood beams. Compos Struct 1997;37(3/4):311–20.
[15] Kollegal MG, Sridharan S. Strength prediction of plain Woven fabrics. J Compos Mater 1998;34:241–57.
[16] Kollegal MG, Sridharan S. A simplified model for plain Woven fabrics. J Compos Mater 1998;34:1757–85.
[17] Trovillion J. Construction Engineering Research Lab, CERL, Urbana-Champagne, Illinois, Private Communication; 2002.
[18] Sikkil KK. Finite element damage modeling of plain weave fabrics. Thesis, Mechanical and Aerospace Engineering, West Virginia University, Morgantown, WV.
[19] Barbero EJ, Luciano R. Formulas for the stiffness of composites with periodic microstructure. Int J Solid Struct 1994;31:2933–43.
[20] Barbero EJ, Luciano R. Micromechanical formulas for the relaxation tensor of linear viscoelastic composites with transversely isotropic fibers. Int J Solid Struct 1995;32:1859–72.
[21] Luciano R, Sacco E. Variational methods for the homogenization of periodic heterogeneous media. Eur J Mech Solids 1998;17(4):599–617.
[22] Abdelal GF, Caceres A, Barbero EJ. A micromechanics damage approach for fatigue of composite materials. J Compos Struct 2002;56:413–22.
[23] Ladeveze P, LeDantec E. Damage modeling of the elementary ply for laminated composites. Compos Sci Technol 1992;43:257–67.
[24] Lonetti P, Barbero EJ, Zinno R, Greco F. Interlaminar damage model for polymer matrix composites. J Compos Mater 2003;37(16):1485–504.
[25] Barbero EJ, Lonetti P. Damage model for composites defined in terms of available data. Mech Compos Mater Struct 2001;8:299–315.
[26] Barbero EJ, Lonetti P. An inelastic damage model for fiber reinforced laminates. J Compos Mater 2002;36:941–62.
[27] Barbero EJ, DeVivo L. A constitutive model for elastic damage in fiber-reinforced PMC laminae. J Damage Mech 2001;10:73–93.
[28] Lemaitre J, Chaboche JL. Mechanics of solid materials. Cambridge, UK: Cambridge University Press; 1990.
[29] ANSYS User Manual, Washington, PA, USA.
[30] Barbero EJ. Prediction of compression strength of unidirectional polymer matrix composites. J Compos Mater 1998;32:483–501.